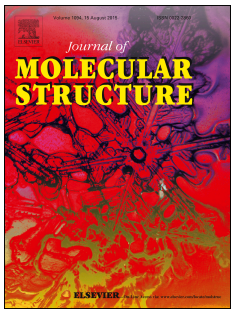

Novel chromenyl-based 2-iminothiazolidin-4-one derivatives as tubulin polymerization inhibitors: Design, synthesis, biological evaluation and molecular modelling studies

Dilep Kumar Sigalapalli, Venkatesh Pooladanda, Manasa Kadagathur, Sravanthi Devi Guggilapu, Jaya Lakshmi Uppu, Chandraiah Godugu, Nagendra Babu Bathini, Neelima D. Tangellamudi

PII: S0022-2860(20)31172-8

DOI: https://doi.org/10.1016/j.molstruc.2020.128847

Reference: MOLSTR 128847

To appear in: *Journal of Molecular Structure*

Received Date: 27 April 2020

Revised Date: 4 July 2020

Accepted Date: 6 July 2020

Please cite this article as: D.K. Sigalapalli, V. Pooladanda, M. Kadagathur, S.D. Guggilapu, J.L. Uppu, C. Godugu, N.B. Bathini, N.D. Tangellamudi, Novel chromenyl-based 2-iminothiazolidin-4-one derivatives as tubulin polymerization inhibitors: Design, synthesis, biological evaluation and molecular modelling studies, *Journal of Molecular Structure* (2020), doi: https://doi.org/10.1016/j.molstruc.2020.128847.

Novel Chromenyl-Based 2-Iminothiazolidin-4-one Derivatives as Tubulin Polymerization Inhibitors: Design, Synthesis, Biological Evaluation and Molecular Modelling Studies

Dileep, Manasa and Sravanthi Devi Guggilapu: Synthesis and characterization

Jaya Lakshmi Uppu: Tubulin assays.

Venkatesh Pooladanda, Chandraiah Godugu: MTT assay

Nagendra Babu Bathini: Concept

Neelima D. Tangellamudi: Concept, Writing, Reviewing and Editing

Graphical Abstract

Novel Chromenyl-Based 2-Iminothiazolidin-4-one Derivatives as Tubulin Polymerization Inhibitors: Design, Synthesis, Biological Evaluation and Molecular Modelling Studies

Dilep Kumar Sigalapalli,[a] Venkatesh Pooladanda,[c] Manasa Kadagathur,[a] Sravanthi Devi Guggilapu,[a,d] Jaya Lakshmi Uppu,[a] Chandraiah Godugu,*[c] Nagendra Babu Bathini,*[b] and Neelima D. Tangellamudi,*[a]

[a] Department of Medicinal Chemistry, National Institute of Pharmaceutical Education and Research (NIPER), Hyderabad 500037, India

[b] Fluoro-Agrochemicals, CSIR-Indian Institute of Chemical Technology, Hyderabad 500007, India

[c] Department of Regulatory Toxicology, National Institute of Pharmaceutical Education and Research (NIPER), Hyderabad 500037, India

[d] Present address: National Institutes of Health, National Institute of Diabetes and Digestive and Kidney Diseases, Laboratory of Bioorganic Chemistry, Bethesda, MD 20892, USA

*[a]Corresponding author. E-mail: tdneelima@gmail.com

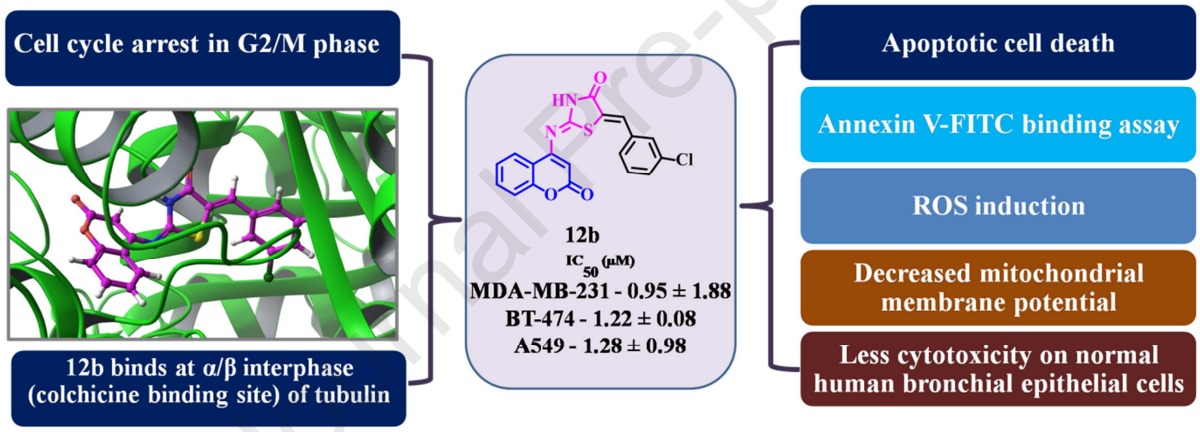

Novel Chromenyl-Based 2-Iminothiazolidin-4-one Derivatives as Tubulin Polymerization Inhibitors: Design, Synthesis, Biological Evaluation and Molecular Modelling Studies

Dilep Kumar Sigalapalli,[a] Venkatesh Pooladanda,[c] Manasa Kadagathur,[a] Sravanthi Devi Guggilapu,[a,d] Jaya Lakshmi Uppu,[a] Chandraiah Godugu,*[c] Nagendra Babu Bathini,*[b] and Neelima D. Tangellamudi,*[a]

[a] Department of Medicinal Chemistry, National Institute of Pharmaceutical Education and Research (NIPER), Hyderabad 500037, India

[b] Fluoro-Agrochemicals, CSIR-Indian Institute of Chemical Technology, Hyderabad 500007, India

[c] Department of Regulatory Toxicology, National Institute of Pharmaceutical Education and Research (NIPER), Hyderabad 500037, India

[d] Present address: National Institutes of Health, National Institute of Diabetes and Digestive and Kidney Diseases, Laboratory of Bioorganic Chemistry, Bethesda, MD 20892, USA

*[a]Corresponding author. E-mail: tdneelima@gmail.com

Abstract

Here-in, we present molecular design, chemical synthesis and evaluation of novel chromenyl-based 2-iminothiazolidin-4-one derivatives as tubulin polymerization inhibitors. The newly synthesized compounds were evaluated for their *in vitro* cytotoxicities against A549 (lung cancer), MDA-MB-231 and BT-471 (breast cancer), HepG2 (liver cancer) and HCT-116 (colon cancer) cell lines by MTT assay. Among the synthesized compounds, compound **12b** showed excellent anticancer activity on MDA-MB-231 cell line with IC_{50} value of 0.95 ± 1.88 µM and was verified to be safe in normal human bronchial epithelial cells (Beas-2B). Apoptosis induced by the lead **12b** was observed using morphological observations, AO/EB and DAPI staining procedures. Further, dose-dependent increase in the depolarization of mitochondrial membrane was also observed through JC-1 staining. Annexin V-FITC/PI assay confirmed that **12b** induced early apoptosis. Additionally, cell cycle analysis indicated that the MDA-MB-231 cells were arrested at sub-G2/M phase and also inhibited tubulin polymerization with IC_{50} value of 3.54 ± 0.2 µM. Molecular docking simulations were employed to identify the important binding modes resposible for the tubulin inhibitory activity, thus supporting their effective anticancer potential.

KEY WORDS: 2-iminothiazolidin-4-one, chromenone, cytotoxicity, tubulin polymerization, apoptosis, molecular modelling.

1. Introduction

Cancer, a complex and heterogeneous disease, that can be defined as growth of cells beyond their usual boundaries is the cause for escalating number of deaths across the globe [1]. It is characterized by unrestricted cell proliferation, division and metastasis that may be attributed to irregular microtubule dynamics [2,3]. Microtubules are the structures with a key role in cell formation, division, cell shape maintenance, intracellular transport, signalling etc [4,5]. The microtubules are comprised of α/β-tubulin heterodimers which fold and unfold to give specific complexes [6]. Any alterations in the conformations of these complexes result in the microtubule catastrophe. Microtubulin interacting drugs, are important agents in cancer chemotherapy which alter microtubule dynamics to arrest cell division in mitosis and deploy a crucial role as chemotherapeutic agents [7,8].

2-iminothiazolidin-4-one nucleus, one of the privileged scaffolds in modern medicinal chemistry is of great pharmaceutical relevance with regard to its potential applications as inhibitors of metalloproteinases [9], COX-2 [10], CDK-2 [11], and SHP-2 [12]. Apart from the pharmacological activities as antidiabetic, anti-inflammatory, anticonvulsant, antimicrobial and antipsychotic agents, 2-iminothiazolidin-4-one has been proven to be a molecule of immense therapeutic interest as an anticancer agent and inhibitors of tubulin assembly of the microtubules [13-17].

A series of 4-thiazolidinone-indolin-2-ones **A** and **B** were reportedly found to be significantly cytotoxic against HT-29, H460, MDA-MB-231 and SMMC-7721 cancer cell lines (IC_{50} = 0.025 μM, 0.075 μM, 0.77 μM, 1.95 μM respectively) [18]. A series of 2-imino thiazolidinones **C** were reported to kill MDA-MB-231cancer cells at an IC_{50} between 0.3 and 6.43 μM [19]. In 2006, substituted 5-benzylidene-2-phenylimino-1,3-thiazolidin-4-one analogs of D that can effectively induce apoptosis in various cancer cells, including paclitaxel- and vinorelbine-sensitive and -resistant human lung cancer cells but not in normal cells, have been reported [20]. Thus, 5-benzylidene-2-phenylimino thiazolidinone moiety has been noted to be responsible for its anti-cancer potential.

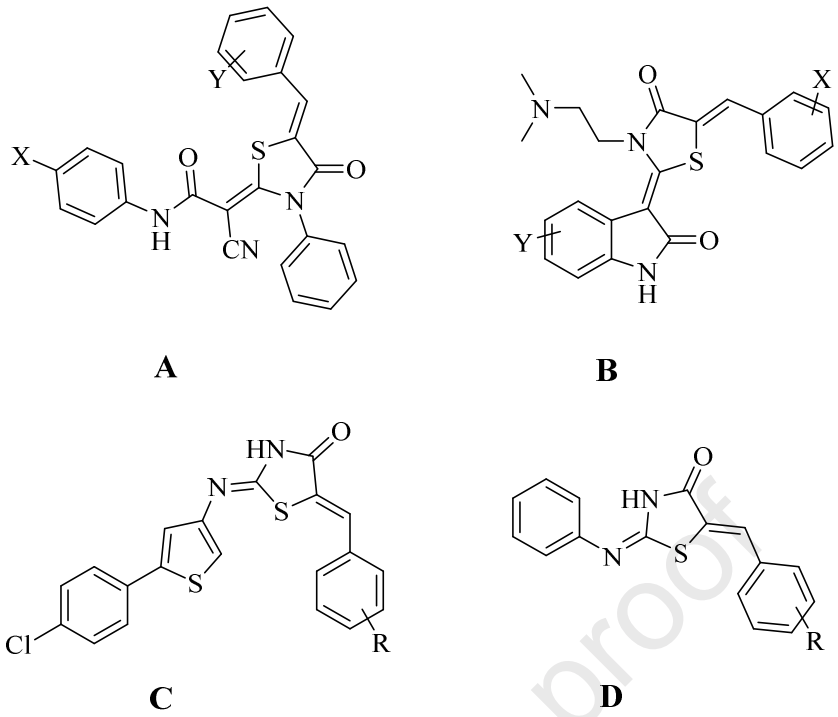

Chart1: Chemical structures of thiazolidinone conjugates with potent anti-proliferative activity on MDA-MB, SMMC-7721 and human lung cancer cells.

Chromene-2-ones and chromene-4-ones, collectively called chromenes, belonging to the family of flavonoids, are known for their natural abundance in the form of quercetin, rutin and luteolin which are known for their therapeutic properties against various diseases [21]. Yi-ming et.al reported novel chromene-2-ones as anticancer agents by targeting microtubule depolymerization and G2-M arrest followed by apoptosis in cancer cell lines [22]. Recently Rasha et.al synthesized new aryl chromene-2-ones as tubulin polymerization inhibitors [23]. Chromene-2-one-hydrazone derivatives were reported as tubulin targeted anticancer agents and 7-Diethylamino chromene-2-one was also reported as a novel microtubule inhibitor with antimitotic activity in multidrug resistant cancer cells [24]. RKS262 and TGX286 are some of the chromene-2-one and chromene-4-one containing compounds respectively which are reported for their vivid anticancer potential. Some of the representative structures of 2-iminothiazolidin-4-one and chromenone core-containing molecules as anti-proliferative agents are depicted in figure 1 [25-28].

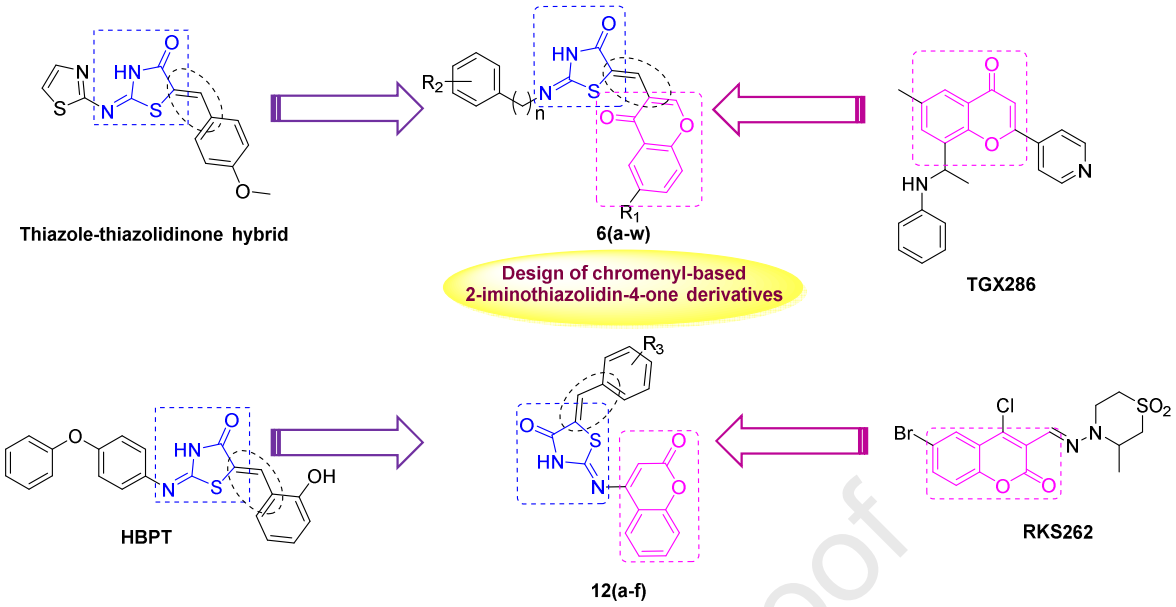

Figure 1. Examples of bioactive 2-iminothiazolidin-4-one and chromenone containing anticancer agents.

Although chemotherapeutic drugs have different modes of action viz, cause DNA damage, interfere with DNA synthesis and inhibit mitotic spindle, drugs that interfere with mitotic spindle formation by tubulin polymerization inhibitors have ben the most successful chemotherapeutic compounds currently used for anti-cancer treatment. In the light of these previous reports on chrome-2-ones as tubulin polymerization inhibitors and anti-proliferative activities of 5-benzylidene 2-iminothiazolidinone moiety in cancer research, and in continuation with our consistent efforts towards the synthesis of cytotoxic NCEs [29-31], we were encouraged to design and synthesize some lead molecules by incorporating chromenes into 2-iminothiazolidinone framework (figure 1) with the primary aim of finding potent newer molecules as tubulin polymerization inhibitors with a better therapeutic profile.

2. Material and Methods

2.1. Chemistry

The reagents and solvents used for the synthesis of designed molecules were obtained from commercial suppliers. MERCK pre-coated silica gel 60-F-254 (0.5 mm) aluminium plates used to perform analytical thin layer chromatography (TLC). Ultraviolet light was used to visualize the spots on TLC plates. Column chromatography was performed using silica gel 60-120. ^{1}H and ^{13}C NMR spectra were recorded on Bruker 500 MHz instrument in $CDCl_3$ or DMSO-d_6 solvents using tetramethylsilane (TMS) as the internal standard. Chemical shifts for ^{1}H and ^{13}C are reported in parts per million (ppm) downfield from tetramethylsilane. Spin multiplicities are described as s (singlet), bs (broad singlet), d (doublet), dd (doublet of

doublets), t (triplet), q (quartet), and m (multiplet). Coupling constant (*J*) values are reported in Hertz (Hz). All IR spectra were recorded on a Perkin Elmer FT-IR spectrometer. HRMS were determined with Agilent QTOF mass spectrometer 6540 series instrument. Melting point was determined with the help of Stuart advanced melting point apparatus. The names of all the compounds given in the supporting information were taken from ChemBioDraw Ultra, Version 12.0.

2.2. Biology

Cell culture

Human cancer cell lines such as lung (A549), breast (MDA-MB-231 and BT-474), liver (HepG2), colon (HCT-116) and normal human bronchial epithelial cells (Beas-2B) were obtained from National Centre for Cell Science, Pune, India. DMEM and RPMI-1640 Medium (Sigma-Aldrich, USA) was used for the culture and growth of procured cell lines. 10% fetal bovine serum stabilized with 1% antibiotic-antimycotic solution (Sigma-Aldrich, USA) was supplied to the cells in incubator at 37 □C. After reaching 80-90% of confluency, cells were further sub-cultured using 0.25% trypsin/1 mM EDTA solution for additional passage.

MTT assay

The anti-proliferative activity of all newly synthesized compounds was determined by using MTT assay, where the reduction of MTT (3-(4,5-dimethylthiazol-2-yl)-2,5-diphenyl tetrazolium bromide) by mitochondrial succinate dehydrogenase was measured. In brief, the cells were allowed for seeding in 96-well plates (4000 cells per well) using 100 µL of medium. Further, the cells were allowed to grow overnight for attachment onto the wells. Then, different concentrations of the synthesized compounds were used to treat cells for a period of 72 h. Later, 100 µL of MTT (0.5 mg/mL) was added and incubated at 37 □C for 4 h. After that, MTT reagent was aspirated and the formazan crystals formed were dissolved in DMSO (200 µL) for the period of 20 min at 37 □C. Finally, the formed formazan was measured by using a spectrophotometric microtiter plate reader at 570 nm wavelength. Initially, anti-proliferative activity of the synthesized compounds was screened by MTT assay at 30 µM concentration. Further, the compounds with IC_{50} value <30 µM was used for the dose dependent studies at different concentrations ranging from 0.78 µM to 30 µM.

2.3. Molecular modelling studies

Maestro10.4 of Schrödinger suite 2015-4 was used to perform molecular modelling studies of the corresponding chromenyl-based 2-iminothiazolidin-4-one derivatives. Maestro Molecule Builder was employed to draw the 3D structures of the compounds and further optimized by

means of LigPrep module of Schrödinger. Finally, 3D structures of the designed compounds were docked at the active site of tubulin protein.

3. Results and Discussion

3.1. Chemistry

The structural diversity was accomplished by introducing different substituted benzyl or phenethyl moieties on the 2-imino group of thiazolidin-4-one with chromene-4-one at 5 position (**6a-w**). This chromene-4-one side arm was designed to act as potential bioactive moiety imparting certain physicochemical properties like lipophilicity and steric effect [32]. The substituents have been also swapped to check if the less bulkier moieties on 5-position would have any positive effect. However, owing to the presence of α,β-unsaturated lactone system introducing a chromene-2-one on the 2-imino group of thiazolidin-4-one was more convenient than chromene-4-one. Thus **12a-f** were designed by introducing the chromene-2-one as a 2-imino substituent and a benzylidine appendage at 5-position (scheme 1).

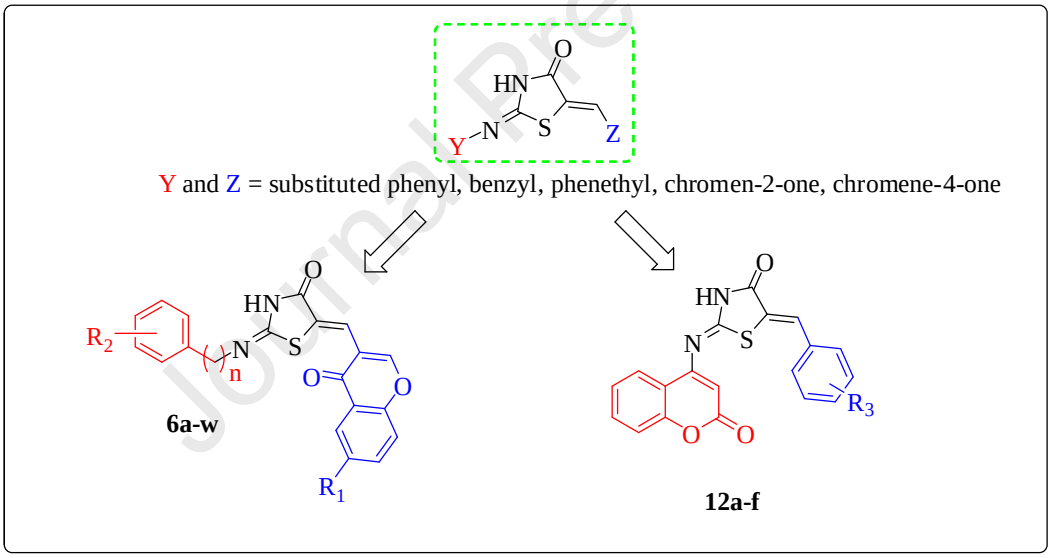

Scheme 1: Design of novel chromene-4-one/ chromene-2-one based molecular hybrids of 2-iminothiazolidin-4-one

The multi-step reaction protocols used to arrive at **6a-w** and **12a-f** series are provided in Scheme 2a and 2b. 2-Iminothiazolidin-4-one **(5)** moiety was synthesized in good to excellent yields by cyclization of corresponding *N*-benzyl/phenethyl-2-chloroacetamide **(4)** which was obtained by chloroacetylation of commercially available benzyl/phenethylamine **(3)** [33]. The required appendage 3-formylchromone **(2)** was synthesized from readily available *o*-hydroxyacetophenone **(1)** under Vilsmeier-Haack reaction conditions ($POCl_3$ in DMF) [34,35]. On the same note, 2-((2-oxo-2*H*-chromen-4-yl)imino)thiazolidin-4-one **(10)** was

obtained by cyclization of chloroacetamide derivative **(9)**, that was synthesized by chloroacetylation of the corresponding 4-aminocoumarin **(8).** 4-Aminocoumarin **(8)** was obtained by simple amination of hydroxycoumarin **(7)** [36]. Finally, 2-iminothiazolidin-4-one (**5** or **10**) was coupled with chromone-3-carbaldehyde/benzaldehyde using sodium acetate in ethanol at 80 □C to furnish the designed target chromenyl-based 2-iminothiazolidin-4-ones (**6a-w** and **12a-f**) in moderate to very good yields (scheme 2a and 2b) [37]. The structures of the obtained compounds (**6a-w** and **12a-f**) were established on the basis of HRMS, ^{1}H and ^{13}C NMR spectroscopy. The ^{1}H NMR spectrum of representative compound **12b** showed a broad singlet of thiazoldinone N-H proton at δ 13.02, singlet of chlorobenzylidene proton at δ 7.74. The sharp singlet of 2*H*-chromene proton appeared at δ 6.11 and rest all protons appeared in the range of δ 7.70-7.35. In the ^{13}C NMR spectrum of **12b**, the carbonyl carbons of thiazoldinone and chromene-2-one appeared at δ 167.72 and 161.21, respectively. The imine carbon of thiazoldinone appeared at δ 158.47. The third carbon of chromene-2-one moiety appeared at δ 101.65 and the remaining carbons appeared in the range of δ 154.35-116.95. Nearly similar patterns were noticed in ^{1}H and ^{13}C NMR spectra of all the compounds (**12a-f**). The HRMS (ESI) of compounds (**6a-w** and **12a-f**) showed characteristic $[M+H]^{+}$ corresponding peaks equivalent to their molecular formulae. The relevant spectral data is furnished in supporting information.

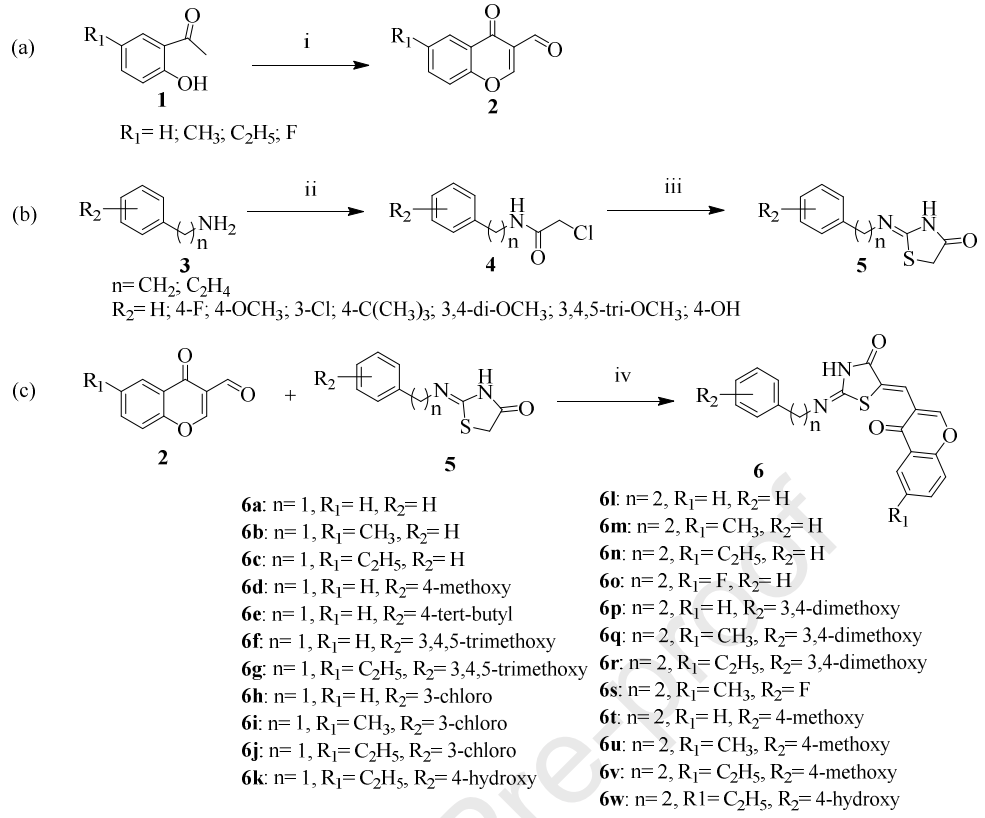

Reagents and conditions: i) DMF/$POCl_3$/80 °C, 12 h ii) DMF/$ClCOCH_2Cl$/0 °C - rt, 4 h (iii) NH_4SCN/ ethyl alcohol/reflux 6 h iv) ethyl alcohol/ piperidine/ reflux 8 h.

Scheme 2a. Synthesis of 2-iminothiazolidin-4-one and chromene-4-one hybrids (**6a-w**).

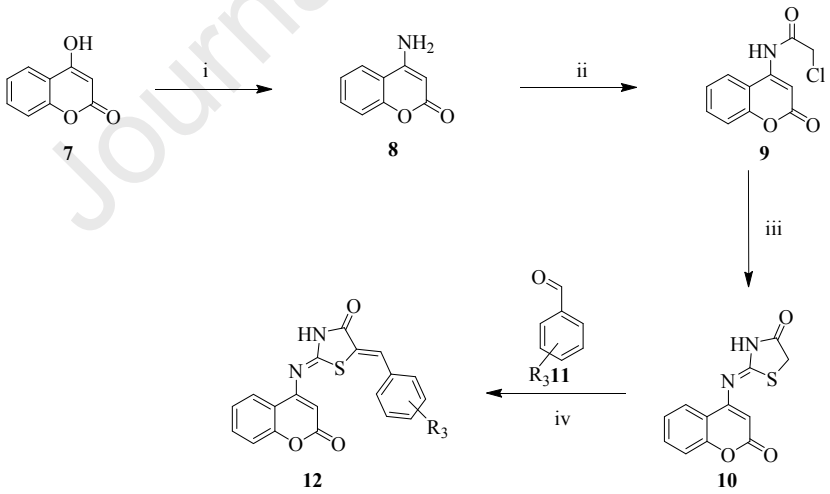

Reagents and conditions: i) ammonium acetate/140 °C, 3 h ii) DMF/$ClCOCH_2Cl$/0 °C - rt, 4 h (iii) NH_4SCN/ ethyl alcohol/reflux 6 h iv) ethyl alcohol/ piperidine/ reflux 8 h

Scheme 2b. Synthesis of 2-iminothiazolidin-4-one and chromene-2-one hybrids (**12a-f**).

The plausible mechanism of the heterocyclization step and the theoretical existence of tautomeric forms of key intermediate 2-iminothiazoldin-4-ones (**5** and **10**) have been shown in scheme 3.

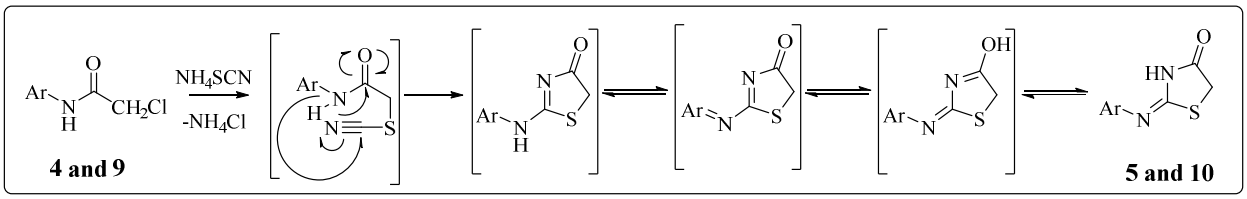

Scheme 3: Mechanistic pathway for 2-iminothiazolidin-4-ones (**5** and **10**) and its tautomers.

Further, the stereochemistry was assigned for one of the representative compounds **12f** by detailed NOE studies. The NOESY experiment was performed for compound **12f** in DMSO-d_6 at 30 □. According to reported literature, *in silico* DFT calculations and NOESY studies revealing the presence of Nuclear Overhauser Effect between H10-H9, H7-H8 and H10-H8 confirms the *Z*-geometry at the double bond as depicted in figure S1, S2 and table S2 (**Supporting information**) [20, 38-41].

3.2. Biological Screening

3.2.1. *In vitro* anti-proliferative activity

MTT (3-(4,5-dimethylthiazol-2-yl)-2,5-diphenyltetrazolium bromide) assay was employed to screen the anti-proliferative activity of all the synthesized compounds (**6a-w** and **12a-f**) on various human cancer cell lines such as lung cancer (A549), breast cancer (MDA-MB-231 and BT-474), liver cancer (HepG2) and colon cancer (HCT-116). The IC_{50} (μM) values of investigational compounds and reference standard (nocodazole) are depicted in table 1.

Table 1. *In vitro* anticancer activity of compounds **6a-w** and **12a-f**.

S. No	Compound	IC_{50} (μM)[a]					
		A549[b]	MDA-MB-231[c]	BT-474[d]	HepG2[e]	HCT-116[f]	Beas-2B[g]
1	6a	>30	>30	>30	>30	>30	-
2	6b	>30	>30	>30	>30	>30	-
3	6c	19.43 ± 0.53	16.90 ± 0.55	18.15 ± 1.12	>30	>30	-
4	6d	23.80 ± 1.13	26.10 ± 1.57	>30	18.12 ± 1.07	24.72 ± 0.64	-
5	6e	>30	>30	>30	>30	>30	-
6	6f	27.11 ± 0.54	>30	19.10 ± 2.10	>30	>30	-
7	6g	21.42 ± 0.80	>30	20.86 ± 0.33	28.98 ± 0.42	27.01 ± 2.14	-
8	6h	16.01 ± 2.18	26.41 ± 2.31	17.88 ± 1.08	>30	>30	-
9	6i	19.21 ± 1.19	17.93 ± 2.90	>30	18.54 ± 1.97	12.03 ± 1.11	-
10	6j	17.38 ± 0.80	18.79 ± 1.42	21.25 ± 0.58	>30	>30	-

11	**6k**	26.89 ± 0.70	29.21 ± 0.23	>30	>30	25.74 ± 0.13	-
12	**6l**	>30	21.47 ± 1.12	>30	>30	>30	-
13	**6m**	>30	>30	>30	>30	>30	-
14	**6n**	26.22 ± 0.76	20.47 ± 1.30	24.80 ± 0.23	18.23 ± 0.16	19.09 ± 0.31	-
15	**6o**	>30	11.89 ± 1.19	>30	15.22 ± 1.158	24.01 ± 0.87	-
16	**6p**	22.17 ± 0.98	19.07 ± 1.08	17.98 ± 0.10	25.28 ± 0.98	28.848 ± 1.54	-
17	**6q**	26.19 ± 1.55	>30	>30	28.90 ± 0.57	20.59 ± 2.01	-
18	**6r**	20.39 ± 0.90	19.88 ± 0.12	29.02 ± 0.30	25.01 ± 1.24	24.12 ± 0.93	-
19	**6s**	19.23 ± 1.53	16.84 ± 0.82	>30	>30	20.98 ± 0.50	-
20	**6t**	>30	>30	>30	>30	>30	-
21	**6u**	>30	14.46 ± 0.18	>30	>30	12.79 ± 2.41	-
22	**6v**	>30	10.27 ± 2.52	>30	15.46 ± 1.42	16.13 ± 1.81	-
23	**6w**	20.34 ± 0.85	>30	>30	>30	>30	-
24	**12a**	>30	>30	26.98 ± 1.76	>30	>30	-
25	**12b**	**1.28 ± 0.98**	**0.95 ± 1.88**	**1.22 ± 0.08**	**30.83 ± 1.48**	**10.14 ± 0.81**	**28.06 ± 1.24**
26	**12c**	15.04 ± 1.77	13.77 ± 0.98	4.65 ± 0.66	>30	19.04 ± 1.01	-
27	**12d**	8.68 ± 0.11	>30	23.94 ± 1.37	8.02 ± 0.96	19.14 ± 0.12	-
28	**12e**	25.90 ± 0.19	28.76 ± 0.18	>30	>30	17.52 ± 0.03	-
29	**12f**	23.58 ± 0.49	>30	21.01 ± 0.75	16.29 ± 1.01	>30	-
30	**Nocodazole**	0.68 ± 0.44	2.68 ± 1.24	1.44 ± 0.14	0. 99 ± 1.87	0.87 ± 1.44	-

[a] 50% Inhibitory concentration after 72 h of drug treatment. [b] Human lung cancer. [c, d] Human breast cancer. [e] Human liver cancer. [f] Human colon cancer. [g] Human normal bronchial epithelium.

The preliminary screening results indicated that some of the synthesized compounds exhibit moderate to potent anti-proliferative activity against the tested cancer cells with IC_{50} values in the range of 0.95 ± 1.88 to 16.13 ± 1.81 μM. From the observation of IC_{50} values of the tested compounds, it is evident that some of the synthesized compounds are sensitive towards lung (A549) and breast (MDA-MB-231 and BT-474) cancer cell lines and some are moderate active on liver (HepG2) and colon (HCT-116) cancer cells. From the MTT assay results we observed that, while compounds **6o**, **6u**, **6v**, **12b**, **12c** and**12d** were the most active, the remaining are moderately active to inactive against the tested cancer cells. Fascinatingly, the compound **12b** was found to be most active in lung (A549) and breast (MDA-MB-231 and BT-474) cell lines and showed discernible anti-proliferative activity with IC_{50} of 0.95 ± 1.88 μM towards MDA-MB-231 cells. Gratifyingly, the compound **12b** was found to be 28-fold less active towards normal human bronchial epithelial cells (Beas-2B) with IC_{50} of 28.06 ± 1.24 μM in contrast to MDA-MB-231 cells, which portrays the selectivity of our synthesized compounds towards cancerous cells. The promising anti-proliferative activity of compound

12b on MDA-MB-231 cells motivated us to further proceed with the mechanistic investigation of cancer cell growth inhibition at cellular level.

2.2.2. Cell cycle analysis

The cytotoxic agents display their activity by arresting the progression of cells at a specific phase in cell cycle. So, cell distribution at different phases of cell cycle was performed by flow cytometry to figure out which phase has been arrested by compound **12b**. MDA-MB-231 cells are treated with different concentrations (0.5, 1, 2.5 µM) of **12b** for about 24 h, followed by fixation with ethanol and staining by propidium iodide and analysed using flow cytometer.

From figure 2, it is clear that there is dose dependent increase in cell population in G2/M phase from 38.62 in control to 59.44, 60.28 and 65.63in 0.5µM, 1µM and 2.5µM, respectively, indicating the arrest at G2/M phase of cell cycle by **12b** in MDA-MB-231 cells.

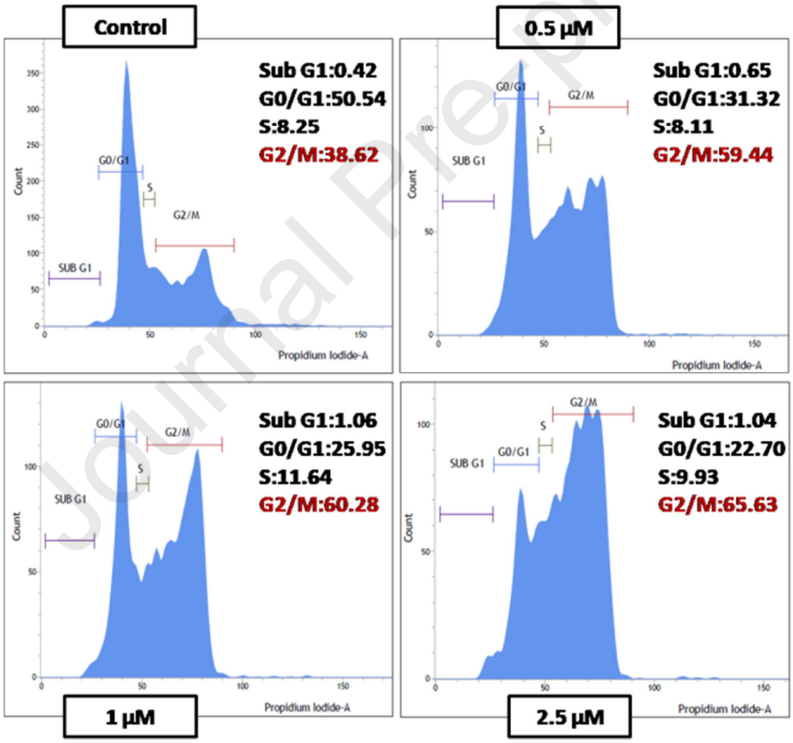

Figure 2. Effect of **12b** on cell cycle progression of MDA-MB-231. Cells were treated with **12b** (0.5, 1 and 2.5 µM) and cell cycle analysis was performed by flow cytometric analysis using PI staining after 24 h of incubation.

3.2.3. Effect on tubulin polymerization

Microtubules are one of the most important components of the eukaryotic cytoskeleton involved in several crucial cellular functions [42,43]. As per the previous literature reports [13,24], 2-iminothiazolidin-4-ones and chromene derivatives are known anti-proliferative

agents that cause inhibition of tubulin polymerization. In the present investigation, a significant inhibition of G2/M phase induced by **12b**, led us to explore its microtubule inhibitory functional aspects. The efficacy of compound **12b** was analysed by studying its effect on tubulin polymerization *in vitro*, with nocodazole as the positive control. Screening at concentrations ranging between 0.31-5 µM revealed that **12b** inhibited the tubulin polymerization in a concentration dependent manner in comparison to nocodazole. At 5 µM concentration, **12b** led to 61.79% percentage of tubulin polymerization inhibition with IC_{50} value of 3.54 ± 0.2 µM. Taken together, the results help us conclude that tubulin might be the molecular target of 2-iminothiazolidin-4-one derivatives.

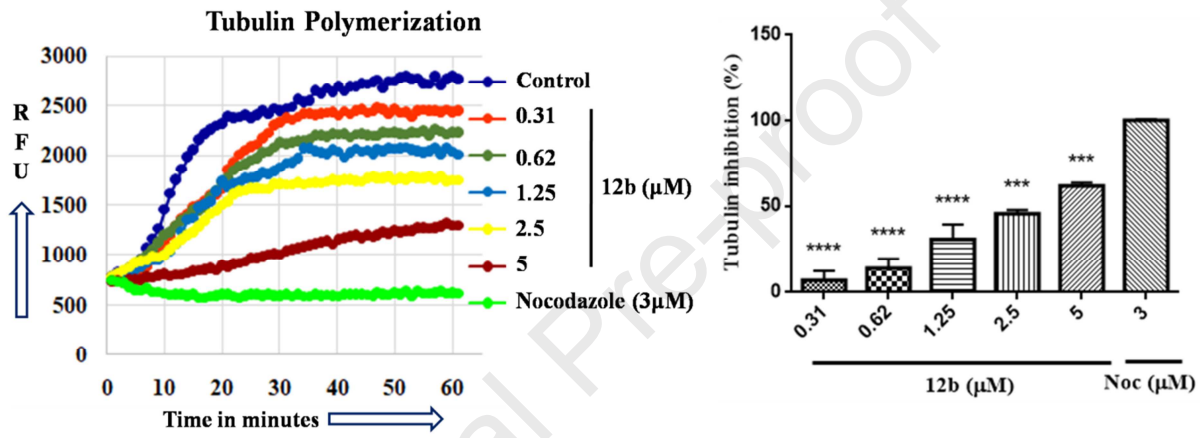

Figure 3. Effect of **12b** on tubulin polymerization. **12b** inhibits the tubulin polymerization in concentration dependent. Here, Noc represents the nocodazole. Data represents as mean ± SEM (n=3). ***p<0.01 and ****p<0.001 are significantly different from nocodazole.

3.2.4. Apoptosis induction studies

In order to investigate the apoptotic-inducing efficiency of **12b** on MDA-MB-231, we have performed AO/EB, DAPI, DCFDA, JC-1 staining, clonogenic growth inhibition and Annexin V binding assays and summarized the results in the description below.

3.2.4.1. Morphological observations using phase contrast microscopy

To uncover the efficiency of the active compound on cellular morphology, MDA-MB-231 cells were treated with **12b** at different concentrations of 0.5, 1 and 2.5 µM for about 48 h. The cells were observed for the changes under phase contrast microscope and the images were captured. From the figure 4, it can be inferred that, increase in concentration of compound resulted in steep decrease in cell viability as compared to control (untreated cells). Additionally, at the higher concentration of 2.5 µM, almost complete diminution of cell number was observed.

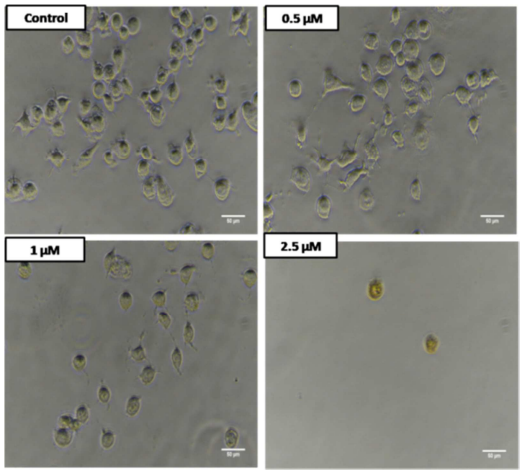

Figure 4. Morphological changes observed in MDA-MB-231cells after treatment with **12b** for 48 h. Images were captured at 200X magnification under phase contrast microscope.

3.2.4.2. AO/EB staining

AO/EB is a dye which efficiently diffuses into the cell membranes of live cells and gives green stain to the nuclei. AO/EB staining assay was performed on MDA-MB-231 following the treatment of cells with **12b** at different concentrations to able to distinguish the live cells from the deceased ones.

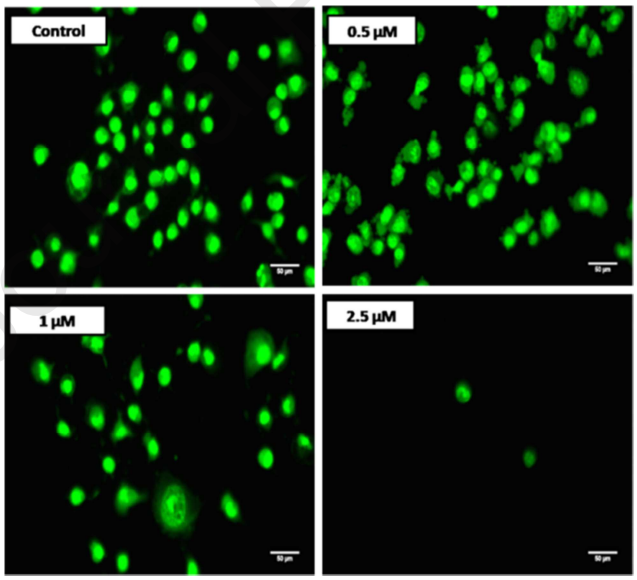

Figure 5. AO/EB staining of **12b**. Cells were treated with **12b** in the concentrations of 0.5, 1 and 2.5 µM and compared with control (DMSO treatment). Images were captured at 200X magnification under fluorescent microscope.

12b was found to cause decrease in live-cell population in dose dependent manner. The assay further enabled us to clearly visualize other characteristic apoptotic features such as cell shrinkage and membrane blebbing (figure 5).

3.2.4.3. DAPI staining

The *in vitro* cytotoxic agents also induce apoptosis by causing nuclear damage and chromatin condensation which can be visualized by a fluorescent stain DAPI (4',6-diamidino-2-phenylindole). While the dye permeates less efficiently into live cell membrane, it has impeccable ability to stain apoptotic cells due to the condensation of nucleus, which is a distinctive feature of the dye exploited in this assay. Thus, DAPI staining was performed on MDA-MB-231 cells following the treatment of cells with different concentrations of **12b.** From figure 6 we inferred that in comparison to control, the nucleus of the cells treated with **12b** took the blue stain, displayed chromatin condensation and horse shoe shaped nuclei in a dose dependent manner.

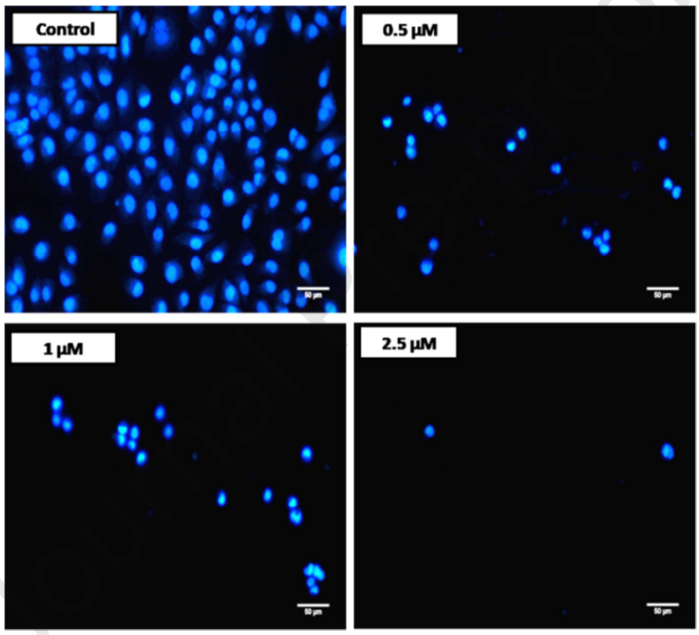

Figure 6. Nuclear morphology of cancer cells after DAPI staining. MDA-MB-231 cells were treated with different concentrations of **12b** for 48 h and stained with DAPI. The images were captured by fluorescence microscope at 200X.

3.2.4.4. DCF fluorescence

ROS (reactive oxidative species) generation is a consistent property in most of the cytotoxic agents. The ROS generation can be analysed in cancer cells using DCF-DA (2',7'-dichlorofluorescin diacetate) assay. To quantify the ability of ROS generation by **12b**, DCF-DA assay was performed on MDA-MB-231 cells treated with **12b** and results are summarized in figure 7**. 12b** induced significant generation of ROS and the clear concentration dependency and quantification in treated cells as compared to control is represented in bar diagram.

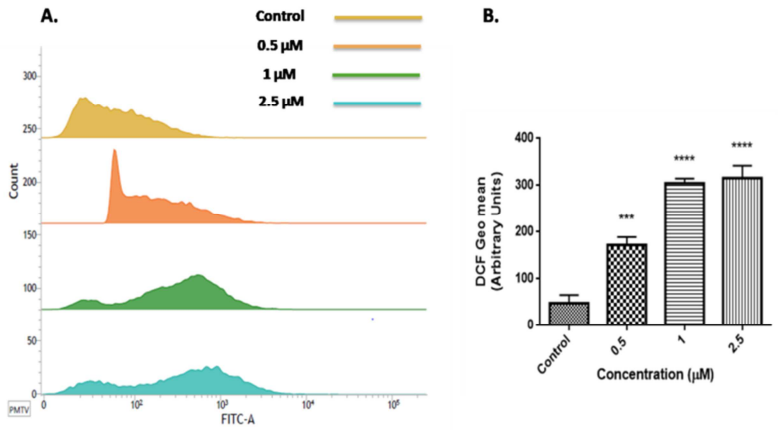

Figure 7. 12b enhances ROS accumulation in cancer cells. (A) MDA-MB-231 cells were treated with **12b** (0.5, 1 and 2.5 µM) for 48 h (B) Relative DCF fluorescence intensity was measured and represented as bar chart.

3.2.4.5. Mitochondrial membrane potential (ΔΨm)

The mitochondria play a vital role in different cellular process and are essential for healthy functioning of cell. Decrease in the mitochondrial membrane potential is observed as a result of cellular oxidative stress mediated by ROS generation *via* inhibition of electron transport chain (ETC). Any disruption in mitochondrial membrane potential is an apparent impact of early apoptosis.

Apparently, ROS generation by **12b** was confirmed by DCF-DA staining assay and JC-1 staining was performed to further quantify and analyse the mitochondrial membrane potential in MDA-MB-231 cells. JC-1 is a lipophilic, cationic dye that stains normal polarised mitochondria in red because of J-aggregates, and depolarised mitochondria in green color due to the presence of J monomers. From the figure 8, it is evident that, with increase in concentration of **12b**, there is a steep fall in number of healthy mitochondria (P1:56.91 in 2.5 µM) and augmentation in depolarised mitochondria (P2:43.91 in 2.5 µM) indicating the collapse of mitochondrial membrane potential (Dψm) in MDA-MB-231 cells.

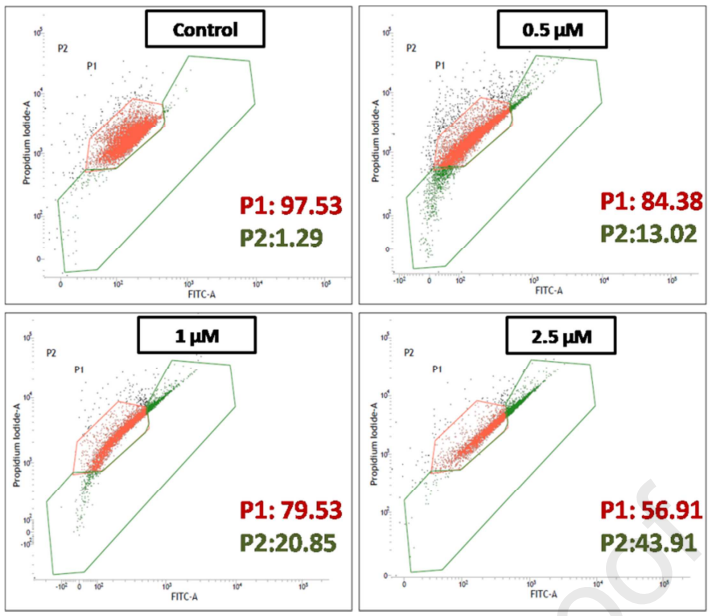

Figure 8. Increased loss of mitochondrial membrane potential (MMP) by **12b** in MDA-MB-231 cells.

3.2.4.6. AnnexinV/Propidium iodide (PI) dual staining assay

Cells were incubated with JC-1 and subjected to flow cytometer for measuring JC-1 aggregates and monomers. Flow cytometric analysis was performed at the concentration of 0.5, 1 and 2.5 µM. Induction of apoptosis by **12b** in MDA-MB-231 cells was confirmed by various staining assays. Therefore to further quantify the extent of apoptosis on MDA-MB-231 cells by **12b**, annexin V –FITC/propidium iodide dual staining assay was performed. This assay has an added advantage of differentiating live (Q1-LL; AV-/PI-), early apoptotic (Q2-LR; AV+/PI-), late apoptotic (Q3-UR; AV+/PI+) and necrotic cells (Q4-UL; AV-/PI+). From the results of figure 9, it can be observed that there is gradual increase in early apoptotic cells in LR quadrant from 2.06 in control to 10.6 in 0.5 µM, 26.49 in 1 µM and 62.75 in 2.5 µM. This reveals the concentration dependent apoptosis induction by **12b** in MDA-MB-231 cells.

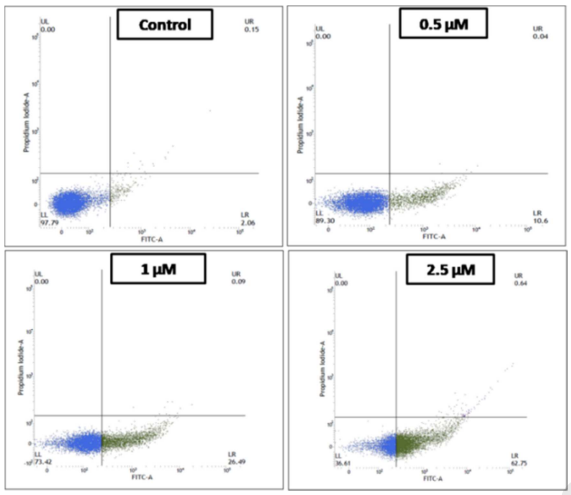

Figure 9. Effect of **12b** on apoptotic cell death in MDA-MB-231 cells after 48 h. **12b** treated cells were stained with Annexin V/PI and analysed for apoptosis using flow cytometer. The 10,000 cells from each sample were analysed by flow cytometry.

3.2.4.7. Clonogenic growth inhibition assay

Colony forming ability of a cancer determines its capability of proliferation and development into solid tumors. A clonogenic assay was performed on MDA-MB-231 cells treated with **12b** at various concentrations (0.5, 1, 2.5 µM) and compared with untreated cells (control). The formation of colonies was observed after 12 days, with an apparent reduction in concentration of treated cells indicating the potency of compound in inhibiting the colony formation (figure 10).

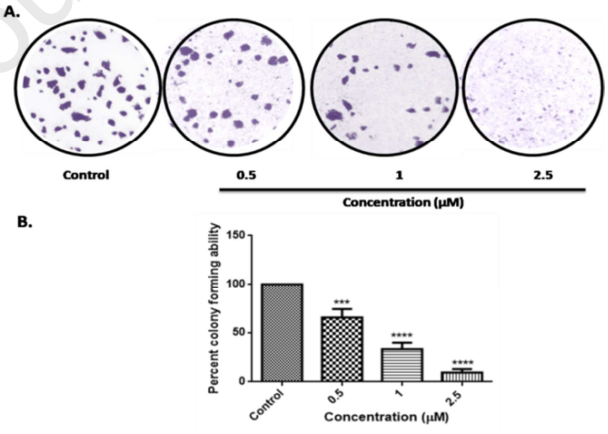

Figure 10. Effect of **12b** on clonogenic growth of MDA-MB-231 cells. Cells were treated with **12b** (0.5, 1 and 2.5 µM) and incubated for 48 h. Further, cells were grown for 12 days and the colonies formed were fixed and stained with 1% crystal violet and photographed using digital camera. (**A**) Clonogenic growth inhibition of **12b** on MDA-MB-231 cells. (**B**) Percentage colonies of MDA-MB-231 cells counted automatically by Vilber Fusion Fx software and data quantified by GraphPad Prism 6.01. The values were expressed as mean ± S.E.M of three similar independent experiments, ***$p<0.001$ and ****$p<0.0001$ versus control.

4. Structure-Activity Relationship (SAR)

The substitutions over benzyl/phenethyl moities on thiazolidinone, and chromenone seem to play a significant role in imparting biological potency. 1) Compounds **6a-c** and **6l-n** with unsubstituted benzyl/phenethyl group on 2-iminothiazolidin-4-one were nearly inactive at 30 μM; 2) The presence of halogen (chloro and fluoro) on benzyl/phenethyl group of thiazolidinone (**6h-j** and **6s**) and chromene-4-one (**6o**) containing compounds resulted in good anti-proliferative activity; 3) Compounds containing electron donating groups such as methoxy and hydroxyl on the benzyl group of thiazolidinone (**6d-g** and **6k**) are nearly less active; 4) Insertion of halogens, chlorine and bromine had a significant effect on IC_{50} values than the corresponding non-halogenated analogues. Specifically, insertion of chlorine resulted in a significant increase in cytotoxic activity compared to the analogue that has bromine. Further, the position of the halogen seemed to be important, as compound **12b**, with chlorine in meta- position of the phenyl is the most potent with an IC_{50} value of 0.9 ± 1.88μM while **12c** with bromine on para- position was the next active compound (13.77 ± 0.98 μM). Surprisingly, **12d** with chlorine in the para- position on the phenyl, however, was less active against MDA-MB cells. Since addition of halogen substituents increase the lipophilicity of a molecule, it might probably assume a bigger size and is more polarized. Overall, the reasonably good IC_{50} values of **12b** and **12c** with chloro and bromo substitutents respectively point towards hydrophobicity and lipophilicity both of which describe the tendency to interact within themselves and other neighbouring moieties; 5) Overall, the *N*-chromenyl-2-one 2-iminothiazolidin-4-ones (scheme 2b) showed greater cytotoxicity than *N*-benzyl/phenethyl 2-iminothiazolidin-4-ones (scheme 2a).

5. Molecular modelling studies

Maestro 10.4 of Schrödinger suite 2015-4 was used to perform molecular modelling studies of the corresponding chromenyl-based 2-iminothiazolidin-4-one derivatives. Maestro Molecule Builder was employed to draw the 3D structures of the compounds and further optimized by means of LigPrep module of Schrödinger. Finally, 3D structures of the designed compounds were docked at the active site of tubulin protein.

5.1. Docking simulation study and Prime MM/GBSA binding energy calculations

The crystal structure coordinates of α/β-tubulin were retrieved from RCSB protein data bank (PDB ID: 1SA0) [44]. Molecular docking simulation studies were performed to elucidate the binding mode and type of interactions of **12b** with α/β-tubulin using GLIDE docking module of Schrödinger suite [45]. This molecular docking simulation study suggested that the top

ranked conformation of **12b** was well accommodated inside the active site of tubulin protein. Figure 11 illustrates the detailed analysis of **12b**-enzyme complex, which reveals the key interactions that appear to play a vital role in the binding of **12b** in the active site of tubulin.

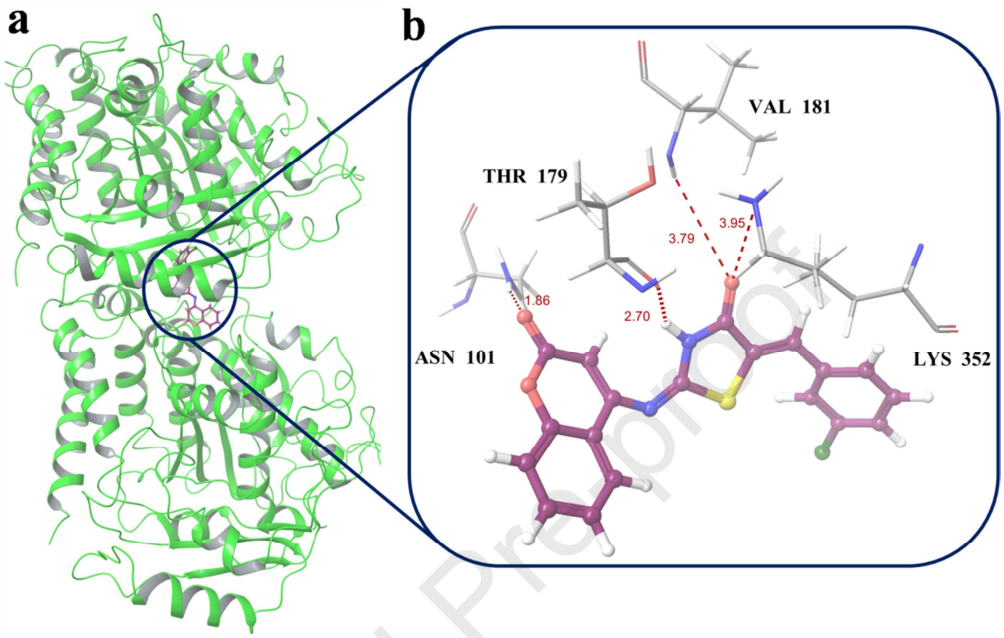

Figure 11. (a) Predicted binding pose of **12b** (ball and stick); (b) Pattern of interactions in the active pocket of α/β tubulin. The red dashed lines represent hydrogen bonds.

12b has shown four hydrogen bond interactions with the active site residues Asn101, Thr179, Val181 and Lys352. In general, **12b** demonstrated a higher H-bond score against the colchicine binding site of α/β-tubulin (Glide H-bond score -0.420 kcal/mol) approximately similar affinity was also observed with the bound ligand (Glide H-bond score -0.511 kcal/mol). The oxygen atom of keto functional group of thiazolidinone moiety has shown H-bond interaction with amino group of Val181, Lys352 with a distance of 3.79 Å and 3.95 Å, respectively. The nitrogen atom of thiazolidinone ring has established one H-bond interaction with the back bone carboxylic acid group of Thr179 (d = 2.70 Å). Similarly, the oxygen atom of keto functional group of chromene scaffold had shown hydrogen bond contact with Asn101 (d = 1.86 Å). Furthermore, **12b** has shown several hydrophobic interactions with the key amino acid residues of α/β tubulin, e.g., Ala180, Val181, Tyr224, Cys241, Leu248, Ala250, Leu255, Ala316, Ala317, Val318, Ala354 and Ile378, these interactions further stabilized the binding of the **12b** in the active site of tubulin.

Figure 12 demonstrates the superimposition of co-crystallized ligand and best docked pose of **12b** in the colchicine binding site of α/β-tubulin. Additionally, binding energy calculations

were also performed on the **12b**-enzyme complex. From the performed studies, we confirmed that **12b** has good binding energy (-49.222 KCal/mol) similar to the nocodazole (-52.761 KCal/mol) and bound ligand (-64.325 KCal/mol), signifying stable ligand-protein complex formation, leading to the stronger binding to the target tubulin protein.

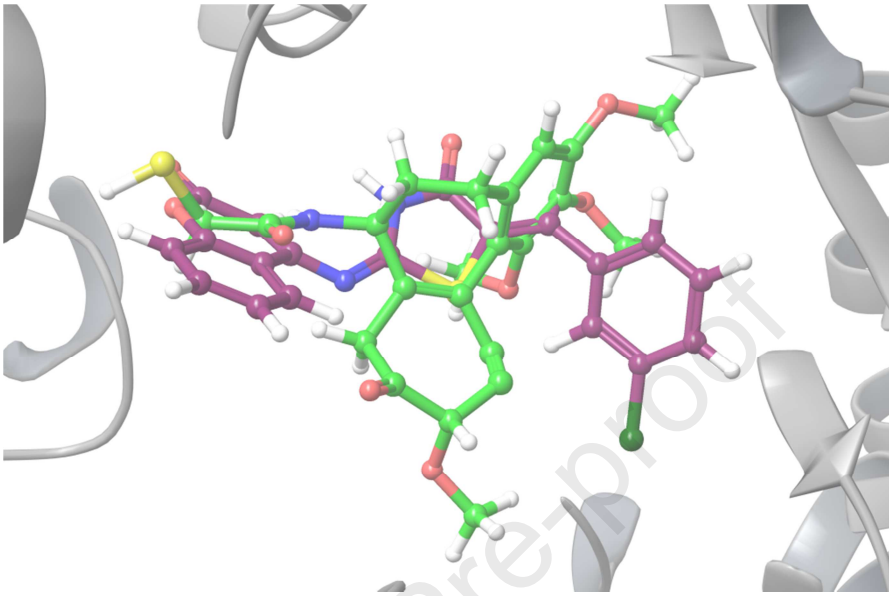

Figure 12. Superimposition of **12b** (maroon colour stick) and co-crystalized ligand (green colour stick) in the colchicine binding site of tubulin.

5.2. *In silico* ADME/T studies

QikProp program of Schrödinger software was used to assess the drug like properties of **12b**. Some of the computed ADME/T parameters are shown in table 2 and their recommended ranges are mentioned. ADME/T prediction studies reveal that, **12b** conforms to the Lipinski's rule of five and has appropriate logP value. Additionally, the recommended ranges of physico-chemical descriptors were also not violated.

Table 2. ADME/T profile of **12b**.

S. No.	ADME/T Parameters	Recommended Values or Range	12b
1	Rule of five	Maximum is 4	No violation
2	PSA (Van der Waals surface area of polar nitrogen and oxygen atoms and carbonyl carbon atoms)	7.0 – 200.0	90.477
3	SASA (Total solvent accessible surface area)	300.0 – 1000.0	623.357
4	Dipole Moment	1.0 – 12.5	8.328
5	Molecular Volume	500.0 – 2000.0	1080.568
6	Donor HB	0.0 – 6.0	1.000

7	Acceptor HB	2.0 – 20.0	6.000
8	QPlogKhsa (Prediction of binding to human serum albumin)	-1.5 – 1.5	0.213
9	QPlogPo/w (Predicted octanol/water partition coefficient)	-2.0 – 6.5	3.376
10	QPpolrz (Predicted polarizability in cubic angstroms)	13.0 – 70.0	38.004
11	QPlogBB (Predicted brain/blood partition coefficient)	-3.0 – 1.2	-0.855
12	QPlogKp (Predicted skin permeability)	-8.0 – -1.0	-2.483
13	QPlogHERG (Predicted IC_{50} value for blockage of HERG K^+ channels.)	concern below -5	-6.233
14	QPPCaco (Predicted apparent Caco-2 cell permeability in nm/sec.)	<25 is poor, >500 great	438.114
15	POA (Predicted human oral absorption on 0 to 100% scale)	>80% is high <25% is poor	93.993

6. Conclusion

In conclusion, we have successfully synthesized, characterized and evaluated different series of chromenyl based 2-iminothiazolidin-4-one derivatives (**6a-w** and **12a-f**) for their anti-cancer potential. Anti-proliferative activities of the synthesized compounds were evaluated in A549 (lung cancer), MDA-MB-231 and BT-474 (breast cancer), HepG2 (liver cancer) and HCT-116 (colon cancer) cell lines using MTT assay. Amongst the synthesized compounds, **12b** showed excellent anti-proliferative activity on all the tested cell lines, particularly in breast cancer cell lines MDA-MB-231, BT-474 (IC_{50} of 0.95 ± 1.88 and 1.22 ± 0.08 μM, respectively) and lung cancer cell line A549 (IC_{50} = 1.28 ± 0.98 μM). The cell cycle analysis disclosed that **12b** showed significant G2/M phase arrest in MDA-MB-231cells. Additionally, **12b** significantly inhibited the tubulin polymerization with IC_{50} value of 3.54 ± 0.2 μM. Further, various mechanistic studies for cell growth inhibition performed on MDA-MB-231 cells, revealed that **12b** caused apoptosis-mediated cell death in MDA-MB-231 cells. The molecular modelling studies inferred that **12b** binds at the colchicine binding site of the tubulin with prominent binding affinity. Furthermore, we have studied physico-chemical and ADMET properties of **12b**, which are in appreciative range. Thus from a practical stand point, chromenyl-2-one based 2-iminothiazolidin-4-one derivatives may lead to the development of potential therapeutic agents with the ability to act on tubulin protein for various aggressive cancers.

Acknowledgment

The authors are thankful to NIPER-Hyderabad for facilities and Department of Pharmaceuticals (DoP), Ministry of Chemicals & Fertilizers, Govt. of India, New Delhi, for the award of NIPER fellowship.

Conflict of Interest

The authors declare no conflict of interest.

References

1. F. Bray, J. Ferlay, I. Soerjomataram, R. L. Siegel, L. A. Torre, A. Jemal, Global cancer statistics 2018: GLOBOCAN estimates of incidence and mortality worldwide for 36 cancers in 185 countries, CA-Cancer J. Clin. 68 (2018) 394-424.
2. C. Dyrager, M. Wickström, M. Fridén-Saxin, A. Friberg, K. Dahlén, E. A. A. Wallén, J. Gullbo, M. Grøtli, K. Luthman, Inhibitors and promoters of tubulin polymerization: Synthesis and biological evaluation of chalcones and related dienonesas potential anticancer agents, Bioorg. Med. Chem. 19 (2011) 2659-2665.
3. M. Borowiak, W. Nahaboo, M. Reynders, K. Nekolla, P. Jalinot, J. Hasserodt, M. Rehberg, M. Delattre, S. Zahler, A. Vollmar, D. Trauner, O. Thorn-Seshold, Photoswitchable inhibitors of microtubule dynamics optically control mitosis and cell death, Cell 162 (2015) 403-411.
4. M. A. Jordan, L. Wilson, Microtubules as a target for anticancer drugs, Nat. Rev. Cancer 4 (2004) 253-265.
5. L. B. Salum, A. Mascarello, R. R. Canevarolo, W. F. Altei, A. B. Laranjeira, P. D. Neuenfeldt, T. R. Stumpf, L. D. Chiaradia-Delatorre, L. L. Vollmer, H. N. Daghestani, C. P. de Souza Melo, A. B. Silveira, P. C. Leal, M. J. Frederico, L. F. do Nascimento, A. R. Santos, A. D. Andricopulo, B. W. Day, R. A. Yunes, A. Vogt, J. A. Yunes, R. J. Nunes, *N*-(1'-naphthyl)-3,4,5-trimethoxybenzohydrazide as microtubule destabilizer: Synthesis, cytotoxicity, inhibition of cell migration and in vivo activity against acute lymphoblastic leukemia, Eur. J. Med. Chem. 96 (2015) 504-518.
6. G. Tian, Y. Huang, H. Rommelaere, J. Vandekerckhove, C. Ampe, N. J. Cowan, Pathway leading to correctly folded β-tubulin, Cell 86 (1996) 287-296.
7. D. Bates, A. Eastman, Microtubule destabilising agents: Far more than just antimitotic anticancer drugs, Br. J. Clin. Pharmacol. 83 (2017) 255-268.

8. E. Mukhtar, V. M. Adhami, H. Mukhtar, Targeting microtubules by natural agents for cancer therapy, Mol. Cancer Ther. 13 (2014) 275-284.
9. L. Crascì, P. Vicini, M. Incerti, V. Cardile, S. Avondo, A. Panico, 2-Benzisothiazolylimino-5-benzylidene-4-thiazolidinones as protective agents against cartilage destruction, Bioorg. Med. Chem. 7 (2015) 1551-1556.
10. K. R. A. Abdellatif, M. A. Abdelgawad, H. A. H. Elshemy, S. S. R. Alsayed, Design, synthesis and biological screening of new 4-thiazolidinone derivatives with promising COX-2 selectivity, anti-inflammatory activity and gastric safety profile, Bioorg. Chem. 64 (2016) 1-12.
11. M. Rashid, A. Husain, M. Shaharyar, R. Mishra, A. Hussain, O. Afzal, Design and synthesis of pyrimidine molecules endowed with thiazolidin-4-one as new anticancer agents, Eur. J. Med. Chem. 83 (2014) 630-645.
12. A. Geronikaki, P. Eleftheriou, P. Vicini, I. Alam, A. Dixit, A. K. Saxena, 2-Thiazolylimino/Heteroarylimino-5-arylidene-4-thiazolidinones as new agents with SHP-2 inhibitory action, J. Med. Chem. 51 (2008) 5221-5228.
13. O. Devinyak, B. Zimenkovsky, R. Lesyk, Biologically active 4-thiazolidinones: A review of QSAR studies and QSAR modeling of antitumor activity, Curr. Top. Med. Chem. 12 (2012) 2763-2784.
14. A. Verma, S.K. Saraf, 4-Thiazolidinone -A biologically active scaffold, Eur. J. Med. Chem. 43 (2008) 897-905.
15. A. C. Tripathi, S. J. Gupta, G. N. Fatima, P. K. Sonar, A. Verma, S. K. Saraf, 4-Thiazolidinones: The advances continue..., Eur. J. Med. Chem. 72 (2014) 52-77.
16. A. K. Jain, A. Vaidya, V. Ravichandran, S. K. Kashaw, R. K. Agrawal, Recent developments and biological activities of thiazolidinone derivatives: A review, Bioorg. Med. Chem. 20 (2012) 3378-3395.
17. a) K. Appalanaidu, R. Kotcherlakota, T. L. Dadmal, V. S. Bollu, R. M. Kumbhare, C. R. Patra, Synthesis and biological evaluation of novel 2-imino-4-thiazolidinone derivatives as potent anti-cancer agents, Bioorg. Med. Chem. Lett. 26 (2016) 5361-5368. b) G. Revelant, S. H. Villaume, S. Dunand, G. Kirsch, H. Schohn, S. Hesse, Synthesis and biological evaluation of novel 2-heteroarylimino-1,3-thiazolidin-4-ones as potential anti-tumor agents, Eur. J. Med. Chem. 94 (2015) 102-112.
18. S. Wang, Y. Zhao, G. Zhang, Y. Lv, N. Zhang, P. Gong, Design, synthesis and biological evaluation of novel 4-thiazolidinones containing indolin-2-one moiety as potential antitumor agent, Eur. J. Med. Chem. 46 (2011) 3509-3518.

19. G. Revelant, S. Huber-Villaume, S. Dunand, G. Kirsch, H. Schohn, S. Hesse, Synthesis and biological evaluation of novel 2-heteroarylimino-1,3-thiazolidin-4-ones as potential anti-tumor agents, Eur. J. Med. Chem. 94 (2015) 102-112.
20. S. Wu, W. Guo, F. Teraishi, J. Pang, K. Kaluarachchi, L. Zhang, J. Davis, F. Dong, B. Yan, B. Fang, Anticancer Activity of 5-Benzylidene-2-Phenylimino-1, 3-Thiazolidin-4-one (BPT) Analogs, Med. Chem. 2 (2006) 597-605.
21. a) S. Khadem, R. J. Marles, Chromone and flavonoid alkaloids: Occurrence and bioactivity, Molecules 17 (2012) 191-206. b) A. V. A. David, R. Arulmoli, S. Parasuraman, Overviews of biological importance of quercetin: A bioactive flavonoid, Pharmacogn. Rev. 10 (2016) 84-89. c) A. Maalik, F. A. Khan, A. Mumtaz, A. Mehmood, S. Azhar, M. Atif, S. Karim, Y. Altaf, I. Tariq, Pharmacological applications of quercetin and its derivatives: A short review, Trop. J. Pharm. Res. 13 (2014) 1561-1566. d) A. Ganeshpurkar, A. K. Saluja, The pharmacological potential of rutin, Saudi Pharm. J. 25 (2017) 149-164. e) Y. Lin, R. Shi, X. Wang, H. M. Shen, Luteolin, a flavonoid with potentials for cancer prevention and therapy, Curr. Cancer Drug Targets 8 (2008) 634-646.
22. M. A. Yi-ming, Z. Yu-bo, X. Chuan-ming, C. Dong-mei, L. Jia, Novel microtubule-targeted agent 6-chloro-4-(methoxyphenyl) coumarin induces G2-M arrest and apoptosis in HeLa cells. Acta Pharmacol. Sin. 33 (2012) 407-417.
23. R. Z. Batran, A. F. Kassem, E. M. H. Abbas, S. A. Elseginy, M. M. Mounier, Design, synthesis and molecular modeling of new 4-phenylcoumarin derivatives as tubulin polymerization inhibitors targeting MCF-7 breast cancer cells, Bioorg. Med. Chem. 26 (2018) 3474-3490.
24. a) G. Pilli, N. Dumala, I. Mattan, P. Grover, M. J. Prakash, Design, synthesis, biological and in silico evaluation of coumarin-hydrazone derivatives as tubulin targeted antiproliferative agents, Bioorg. Chem. 91 (2019) 103143. b) S. N. Kim, N. H. Kim, Y. S. Park, H. Kim, S. Lee, Q. Wang, Y. K. Kim, 7-Diethylamino-3(2'-benzoxazolyl)-coumarin is a novel microtubule inhibitor with antimitotic activity in multidrug resistant cancer cells, Biochem. Pharmacol. 77 (2009) 1773-1779
25. Q. Zhang, X. Liu, X. Li, C. Li, H. Zhou, B. Yan, Antitumor activity of (2E,5Z)-5-(2-hydroxybenzylidene)-2-((4-phenoxyphenyl)imino) thiazolidin-4-one, a novel microtubule-depolymerizing agent, in U87MG human glioblastoma cells and corresponding mouse xenograft model, J. Pharmacol. Sci. 122 (2013) 223-231.

26. A. Geronikaki, P. Eleftheriou, P. Vicini, I. Alam, A. Dixit, A. K. Saxena, 2-Thiazolylimino/heteroarylimino-5-arylidene-4-thiazolidinones as new agents with SHP-2 inhibitory action, J. Med. Chem. 51 (2008) 5221-5228.
27. R. K. Singh, T. S. Lange, K. K. Kim, L. Brard, A coumarin derivative (RKS262) inhibits cell-cycle progression, causes pro-apoptotic signaling and cytotoxicity in ovarian cancer cells, Invest. New Drugs, 29 (2011) 63-72.
28. A. Gaspar, M. J. Matos, J. Garrido, E. Uriarte, F. Borges,Chromone: A valid scaffold in medicinal chemistry, Chem. Rev. 114 (2014) 4960-4992.
29. S. D. Guggilapu, L. Guntuku, T. S. Reddy, A. Nagarsenkar, D. K. Sigalapalli, V. G. M. Naidu, S. K. Bhargava, N. B. Bathini, Synthesis of thiazole linked indolyl-3-glyoxylamide derivatives as tubulin polymerization inhibitors, Eur. J. Med. Chem. 138 (2017) 83-95.
30. P. V. S. Ramya, L. Guntuku, S. Angapelly, C. S. Digwal, U. J. Lakshmi, D. K. Sigalapalli, B. N. Babu, V. G. M. Naidu, A. Kamal, Synthesis and biological evaluation of curcumin inspired imidazo[1,2-a]pyridine analogues as tubulin polymerization inhibitors, Eur. J. Med. Chem. 143 (2018) 216-231.
31. a) N. D. Tangellamudi, S. B. Shinde, V. Pooladanda, C. Godugu, S. Balasubramanian, Facile synthesis of 2-aryl 5-hydroxy benzo[*d*]oxazoles and their *in vitro* anti-proliferative effects on various cancer cell lines, Bioorg. Med. Chem. Lett. 28 (2018) 3639-3647. b) D. K. Sigalapalli, V. Pooladanda, P. Singh, M. Kadagathur, S. D. Guggilapu, J. L. Uppu, N. D. Tangellamudi, P. K. Gangireddy, C. Godugu, N. B. Bathini, Discovery of certain benzyl/phenethylthiazolidinone-indole hybrids as potential anti-proliferative agents: Synthesis, molecular modeling and tubulin polymerization inhibition study, Bioorg. Chem. 92 (2019) 1031883.
32. a) P. Vicini, F. Zani, P. Cossini, I. Doytchinova, Hydrazones of 1,2-benzisothiazole hydrazides: synthesis, antimicrobial activity and QSAR investigations, Eur. J. Med. Chem. 37 (2002) 553-564. b) R. Ottana, R. Maccari, M. L. Barreca, 5-Arylidene-2-imino-4-thiazolidinones: Design and synthesis of novel anti-inflammatory agents, Bioorg. Med. Chem. 13 (2005) 4243-4252. c) A. A. Chavan, N. R. Pai, Synthesis and antimicrobial screening of 5-arylidene-2-imino-4-thiazolidinones, Arkivoc **xvi** (2007) 148-155.
33. R. Ranga, V. Sharma, V. Kumar, New thiazolidinyl analogs containing pyridine ring: Synthesis, biological evaluation and QSAR studies, Med. Chem. Res., 22 (2013) 1538-1548.

34. R. Kanada, M. Tanabe, R. Muromoto, Y. Sato, T. Kuwahara, H. Fukuda, M. Arisawa, T. Matsuda, M. Watanabe, S. Shuto, Synthesis of chiral cis-cyclopropane bearing indole and chromone as potential TNFα inhibitors, J. Org. Chem. 83 (2018) 7672-7682.
35. S. Nazreen, M. S. Alam, H. Hamid, M. S. Yar, A. Dhulap, P. Alam, M. A. Q. Pasha, S. Bano, M. M. Alam, S. Haider, C. Kharbanda, Y. Ali, K. K. Pillai, Thiazolidine-2,4-diones derivatives as PPAR-γ agonists: Synthesis, molecular docking, *in vitro* and *in vivo* antidiabetic activity with hepatotoxicity risk evaluation and effect on PPAR-γ gene expression, Bioorg. Med. Chem. Lett. 24 (2014) 3034-3042.
36. C. j. Hua, K. Zhang, M. Xin, T. Ying, J. Gao, J. Jia, Y. Li, High quantum yield and pH sensitive fluorescence dyes based on coumarin derivatives: Fluorescence characteristics and theoretical study, RSC Adv. 6 (2016) 49221-49227.
37. C. M. Bhalgat, P. V. Darda, K. G. Bothara, S. V. Bhandari, J. Gandhi, B. Ramesh, Synthesis and pharmacological screening of some novel anti-hypertensive agents possessing 5-benzylidene-2-(phenylimino)-thiazolidin-4-one ring, Eur. J. Med. Chem. 76 (2014) 580-588.
38. M. H. Bolli, S. Abele, C. Binkert, R. Bravo, S. Buchmann, D. Bur, J. Gatfield, P. Hess, C. Kohl, C. Mangold, B. Mathys, K. Menyhart, C. Müller, O. Nayler, M. Scherz, G. Schmidt, V. Sippel, B. Steiner, D. Strasser, A. Treiber, T. Weller, 2-Imino-thiazolidin-4-one derivatives as potent, orally active $S1P_1$ receptor agonists, J. Med. Chem. 53 (2010) 4198-4211.
39. Y. B. Wagh, A. S. Kuwar, D. R. Patil, Y. A. Tayade, A. D. Jangale, S. S. Terdale, D. R. Trivedi, J. Gallucci, D. S. Dalal, Highly efficient regioselective synthesis of 2-imino-4-oxothiazolidin-5-ylidene acetates *via* a substitution-dependent cyclization sequence under catalyst-free conditions at ambient temperature, Ind. Eng. Chem. Res. 54 (2015) 9675-9682.
40. D. Havrylyuk, O. Roman, R. Lesyk, Synthetic approaches, structure activity relationship and biological applications for pharmacologically attractive pyrazole/pyrazoline-thiazolidine-based hybrids, Eur. J. Med. Chem.113 (2016) 145-166.
41. Ö. Poyraz, V. U. Jeankumar, S. Saxena, R. Schnell, M. Haraldsson, P. Yogeeswari, D. Sriram, G. Schneider, Structure-guided design of novel thiazolidine inhibitors of o□acetyl serine sulfhydrylase from *mycobacterium tuberculosis,* J. Med. Chem. 56 (2013) 6457-6466.
42. A. E. Prota , K. Bargsten , J. F. Diaz, M. Marsh , C. Cuevas, M. Liniger, C. Neuhaus, J. M. Andreu, K. Altmann, M. O. Steinmetz, A new tubulin-binding site and

pharmacophore for microtubule-destabilizing anticancer drugs, Proc. Natl. Acad. Sci. U. S. A. 111 (2014) 13817-13821.

43. E. Hamel, C. M. Lin, Glutamate-induced polymerization of tubulin: Characteristics of the reaction and application to the large-scale purification of tubulin, Arch. Biochem. Biophys. 209 (1981) 29-40.
44. R.B. Ravelli, B. Gigant, P.A. Curmi, I. Jourdain, S. Lachkar, A. Sobel, M. Knossow, Insight into tubulin regulation from a complex with colchicine and a stathmin-like domain, Nature 428 (2004) 198-202.
45. Schrödinger Suite 2015-4, Schrödinger, LLC, New York (2015).

Research Highlights

- The new chromenyl-based 2-iminothiazolidin-4-one derivatives were synthesized.
- Synthesized compounds displayed significant anti-proliferative activity on different human cancer cell lines.
- Compound **12b** induced apoptosis and cell cycle arrest in G2/M phase in MDA-MB-231 cancer cells and also inhibited tubulin polymerization with IC_{50} value of 3.54 ± 0.2 µM.
- **12b** was almost 28-fold more selective on MDA-MB-231 cells compared to Beas-2B cells.
- Further, a molecular docking analysis was performed on lead compound to identify important binding modes responsible for inhibition activity of tubulin protein.

Declaration of interests

- ✓ ☐The authors declare that they have no known competing financialinterestsor personal relationships that could have appeared to influence the work reported in this paper.

  ☐The authors declare the following financial interests/personal relationships which may be considered as potential competing interests: